Materials Horizons

ROYAL SOCIETY OF CHEMISTRY

COMMUNICATION

View Article Online
View Journal | View Issue

Cite this: *Mater. Horiz.*, 2025, **12**, 3144

Received 16th November 2024,
Accepted 22nd January 2025

DOI: 10.1039/d4mh01648c

rsc.li/materials-horizons

Multi-functional smart bulk hydrogel panels with strong near-infrared shielding and active local control†

Yitong Ding,[ab] Gang Li,[c] Keunhyuk Ryu,[d] JianGuo Guan,[c] Shancheng Wang,[d] Ying Xiong,*[b] Shaoyun Guo[b] and Yi Long*[d]

Thermochromic hydrogel is a versatile smart material that can be used in various applications. In this paper, we present a new concept of smart windows to passively regulate light transmittance and reduce energy consumption while functioning as an information display. By incorporating passive solar regulation and active local control, this window is devised through the multilayer assembly of tailored poly(*N*-isopropylacrylamide) (PNIPAM) hydrogels and surface-modified photonic crystal films. The modified surface tension of solvent tunes the scattering center size of the hydrogel, and the addition of the photothermal films (PT films) imparts a high near-infrared (NIR) shielding and light-to-heat conversion, which is needed for low-latitude smart window application. Together with high writing speed, clarity, and repeatability for local writing. This new smart hydrogel engineering can have broad applications, allowing more functionalities in designing building façades.

New concepts

We introduce a new concept of smart bulk hydrogel panels with strong near-infrared (NIR) shielding. The new designs are created through the multilayer assembly of surface-modified photonic crystal photothermal films and tailored poly(*N*-isopropylacrylamide) (PNIPAM) bulk hydrogels. The NIR selective shielding of the former material, coupled with the enhanced smart NIR modulation performance of the latter, imparts an impressive shielding capability for NIR of nearly 99%. Unlike microgels, bulk hydrogels possess mechanical integrity but enhancing their NIR shielding capability remains challenging. Increasing the thickness or polymer proportion is arguably the most effective approach to enhancing their NIR shielding performance. However, unrestricted increase in polymer thickness or proportion impacts the phase transition speed, potentially compromising its "smart" attributes. Thanks to this technology, we demonstrate that bulk PNIPAM panels can exhibit high NIR shielding capabilities while maintaining smart modulation of visible light. Additionally, this newly engineered hydrogel panel enables active local control, offering enhanced functionality in smart information displays.

1. Introduction

Energy consumption in buildings is generally 40% in developed countries, and windows are the least energy-efficient part.[1–3] Smart windows are one of the most active energy-saving research interests in the last decade.[4–8] Thermochromic hydrogel panels with a passive solar regulation range (280–2500 nm) have garnered interest as smart windows.[9–12] Hydrogels investigated the most for use in smart windows are bulk hydrogels and microgels. The former is a highly polymeric crosslinked network with water that gives a gelish characteristic.[11,13] The latter has a microsphere hydrogel size ranging from tens of nanometers to several microns in water.[14–17] Bulk hydrogels have the advantage of simple fabrication, but they exhibit the disadvantage of limited near-infrared (NIR, 780–2500 nm) shielding capability, which could restrict their potential applications in low-latitude smart windows.[11,18,19]

Thermal radiation within the NIR range constitutes above 50% of the total solar energy, thus the potential for reducing energy consumption for cooling through the utilization of thermochromic hydrogel panels possessing weak NIR shielding is limited.[18,20,21] For microgels, the application of Mie scattering theory to regulate their size is an effective strategy for increasing NIR shielding up to 94%.[15] However, the liquid state poses

[a] *Key Laboratory of Biobased Polymer Materials, Shandong Provincial Education Department, College of Polymer Science and Engineering, Qingdao University of Science and Technology, Qingdao, China*
[b] *State Key Laboratory of Polymer Materials Engineering, Sichuan Provincial Engineering Laboratory of Plastic/Rubber Complex Processing Technology, Polymer Research Institute of Sichuan University, Chengdu 610065, China. E-mail: xiongying@scu.edu.cn*
[c] *State Key Laboratory of Advanced Technology for Materials Synthesis and Processing, International School of Materials Science and Engineering, Wuhan University of Technology, Wuhan 430070, China*
[d] *Department of Electronic Engineering, The Chinese University of Hong Kong, Shatin, New Territories, Hong Kong SAR 999077, China. E-mail: yilong@cuhk.edu.hk*

† Electronic supplementary information (ESI) available. See DOI: https://doi.org/10.1039/d4mh01648c

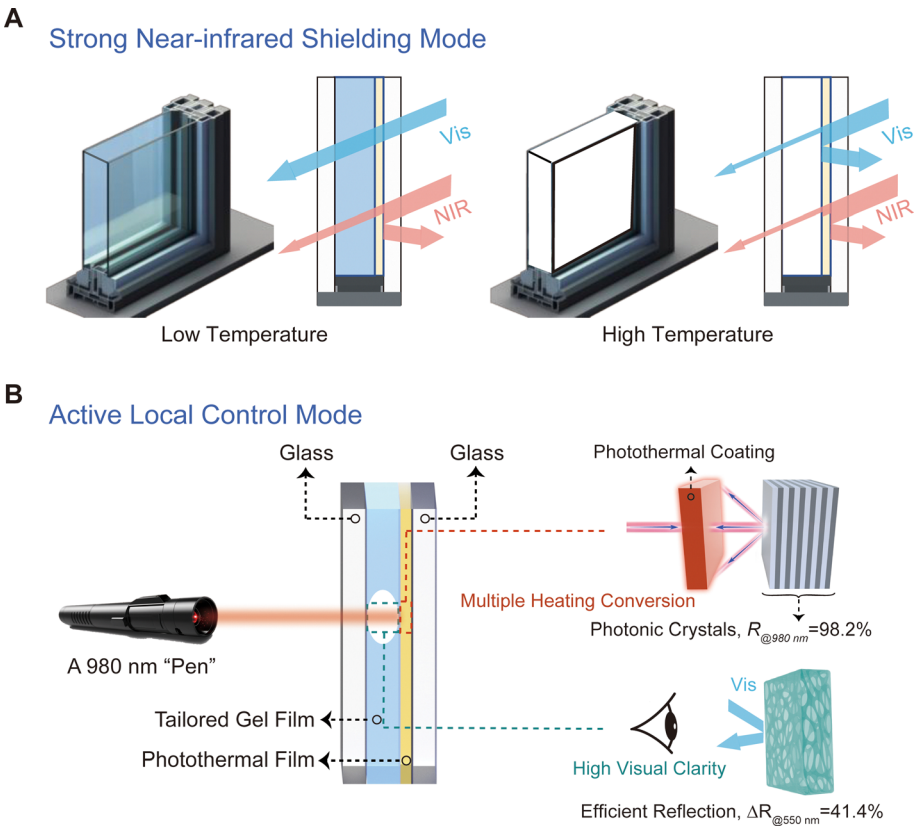

Scheme 1 Design scheme for smart bulk hydrogel panels using (A) strong near-infrared shielding mode and (B) active local control mode.

potential leakage issues. For bulk hydrogels, increasing the thickness or polymer proportion is arguably an effective approach to enhance their NIR shielding performance,[18] accompanied by a compromised phase transition speed.

In this work, a novel approach was employed by combining tailored poly(*N*-isopropylacrylamide) (PNIPAM) hydrogels with surface-modified photonic crystal photothermal films (PT films). This combination enables the development of smart bulk hydrogel panels with strong NIR shielding properties; these panels hold the promise of acting as smart windows to reduce building energy consumption in low-latitude regions. PT films exhibit robust selective NIR shielding, and tailored PNIPAM hydrogels improve their capacity for smart NIR control after solvent-assisted modification, resulting in a composite panel smart window that achieves nearly 99% NIR shielding (Scheme 1A). Moreover, the hydrogel panel designed here can also function as a local writing platform using a NIR laser pen (Scheme 1B). The photonic crystal structure[22] within the PT films can be targeted to reflect NIR (*e.g.*, $R_{@980nm}$, 98.2%), ensuring a high NIR photothermal conversion. In local writing mode, the contrast of reflectivity for 550 nm ($R_{@550nm}$) between the local phase-transitioned area and the rest of the window increased from 35.5 to 41.4% as compared with the unmodified hydrogel panel. This innovative design offers valuable guidance for extending the applications of thermochromic hydrogels in low-latitude smart windows that can potentially work as smart information displays.

2. Experimental section

2.1. Materials

N-Isopropylacrylamide (NIPAM, 98.0%) was purchased by Tokyo Chemical Industry Co., Ltd. *N*,*N*-Methylenebisacrylamide (BIS, 98.5%) and ethanol (99.7%) were bought from Chengdu Kelon Chemical Reagent Factory. 2,2-Diethoxyacetophenone (photoinitiator, 98%) was supplied from Adamas. The NIR PT films were bought from 3 M, Minnesota, USA.

2.2. Preparation of hydrogel panels for light management

The gel panels/molds were prepared as illustrated in Fig. S1 (ESI†). NIPAm (1 g), BIS (10 mg), and photoinitiator (7.5 μl) were dissolved in a mixture (20 ml) of deionized water and ethanol, where the molar content (volumes) of ethanol was 0% (0 ml), 2% (1.2 ml), and 4% (2.4 ml), respectively. After 10 min of nitrogen atmosphere, the sandwich structure (glass-solution-PT film/glass) precursor was prepared using the casting method. Finally, the sandwich structure bulk gel panel (glass-gel-PT film/glass) was polymerized in a UV LED reactor (Shengju Machinery Automation (Shanghai) Co., Ltd, China) under 10% power (10 min, 20 °C) with nitrogen atmosphere. Notably, the gels prepared by this strategy were bulk gels with mechanical integrity (Fig. S2, ESI†). The gel panel without PT film was prepared as a control using the same method. The nomenclature of light management panels/molds (X-PT-Y) and PT films (PT-Y) indicates the types of gels (X), the PT films (PT),

and the different testing directions (Y) (Fig. S3, ESI†). "PNIPAM", "TP-0.02", and "TP-0.04" refer to pure PNIPAM gels, modified PNIPAM gels with 2% ethanol, and modified PNIPAM gels with 4% ethanol, respectively. "−0" and "−1" represent different surfaces of the PT film, respectively. "−0" represents the direction of the photonic crystal layer. "−1" represents the direction of the photothermal coating.

2.3. Characterization

All experimental details are included in the ESI.†

3. Results and discussion

3.1. Strong NIR shielding mode for low-latitude smart windows

Thermochromic bulk hydrogel panels based on poly(*N*-isopropylacrylamide) (PNIPAM) experience transparent-to-translucent transition at a low critical solution temperature (LCST) of ~32 °C. However, when used as a smart window, the regulatory effect on near-infrared light (NIR, 780–2500 nm) is relatively subtle.[23,24] A stronger NIR shielding capability is needed to meet the demands of tropical climates. For this

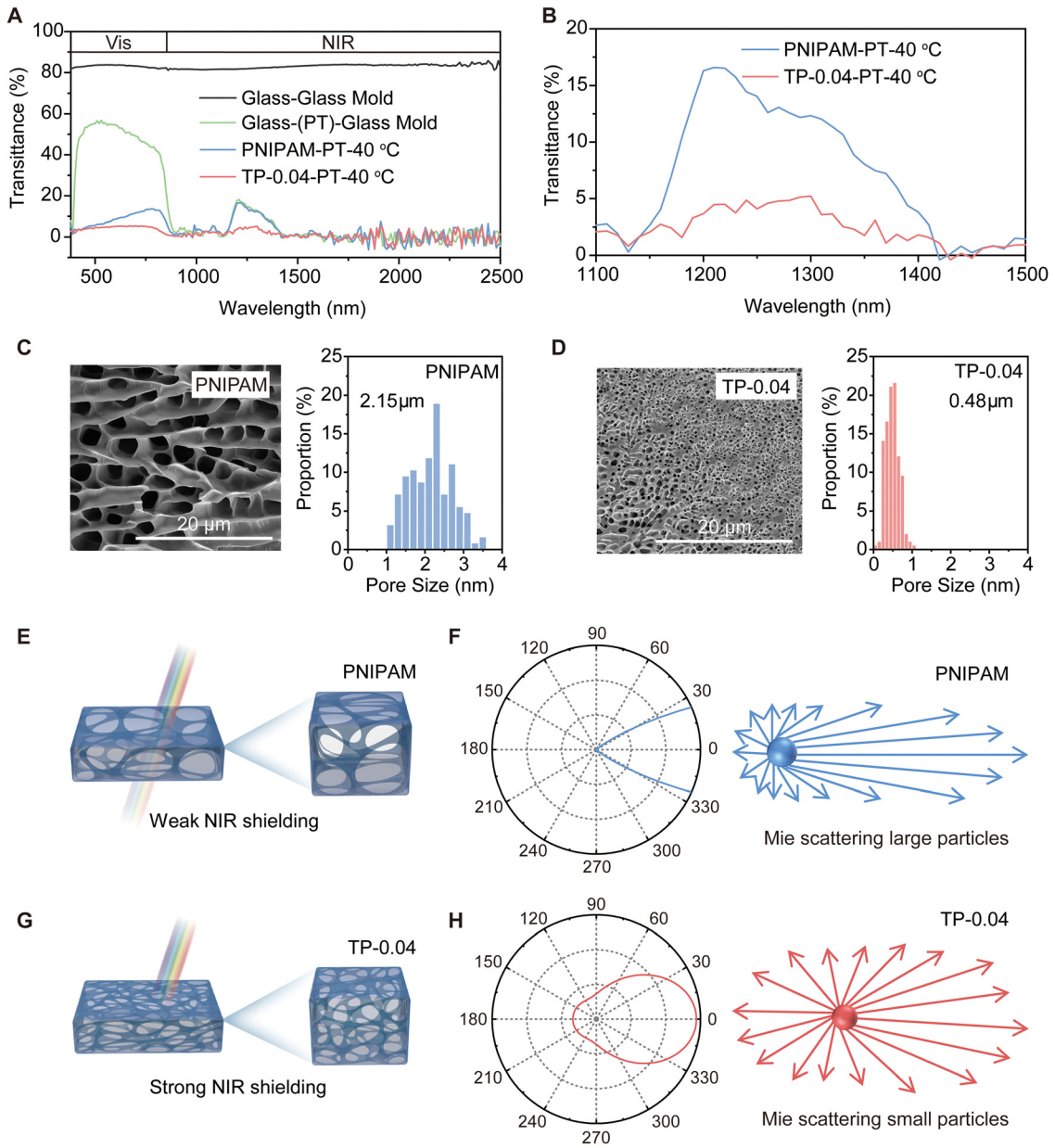

Fig. 1 The NIR shielding performance of the smart bulk hydrogel panel developed here. (A) Vis-NIR transmittance curves of the different panels. (B) Transmittance curves of PNIPAM-PT and TP-0.04-PT smart panels in the 1100–1500 nm band. Scanning electron microscopy (SEM) images of hydrogels and pore size distribution of (C) PNIPAM hydrogel (pristine PNIPAM) and (D) TP-0.04 hydrogel (co-solvent-modified PNIPAM with 4% ethanol) at 60 °C. Schematic diagrams of scattering ((E) PNIPAM and (G) TP-0.04) and the Mie scattering behavior ((F) PNIPAM and (H) TP-0.04) of individual scattering microspheres for 1250 nm light.

purpose, the PT films and cosolvent-modified PNIPAM bulk hydrogels are chosen. As shown in Fig. 1A, the composite mold (glass-(PT)-glass mold) gains the capability to selectively shield NIR after affixing the PT film to the glass mold (glass-glass mold). The cosolvent-modified PNIPAM hydrogels enhance the NIR shielding of the hydrogel panels (Fig. 1A), especially in the 1100–1500 nm range (Fig. 1B). As compared with pristine PNIPAM-PT film composite hydrogel panel (PNIPAM-PT), the transmittance of the cosolvent-modified PNIPAM with 4% ethanol-PT film composite hydrogel panel (TP-0.04-PT) at 1250 nm dropped from ~12% to less than 5%. When the ambient temperature surpassed the LCST, the NIR shielding capability of TP-0.04-PT was ~99%.

The theoretical foundation for the enhanced NIR shielding ability of the PNIPAM bulk gel using cosolvent lies in its phase change mechanism and the Tate law.[11,25] The cosolvent has the ability to decrease the size of scattering microsphere droplets after phase change (above the LCST). This is a phenomenon that is discernible through the micropore size observed in scanning electron microscopy (SEM) (Fig. 1C, D and Fig. S4, ESI†).[26] Compared with the pristine PNIPAM hydrogel, the average micropore size of the cosolvent-modified PNIPAM with 4% ethanol (TP-0.04) decreased from 2.15 to 0.48 μm. Drawing from the Mie scattering theory, alterations in the size of the scattering microsphere droplets significantly enhance the capacity to shield against NIR (Fig. 1E–H).[15,27,28] The Mie scattering response of single scattering microsphere droplets under 1250 nm light was calculated and compared (Fig. 1F and H). For the pristine PNIPAM hydrogel, the forward scattering (0–90° and 270–360°) of individual microspheres is highly pronounced, whereas backward scattering (90–270°) is not as evident (Fig. 1F). Upon introducing the cosolvent, there is a

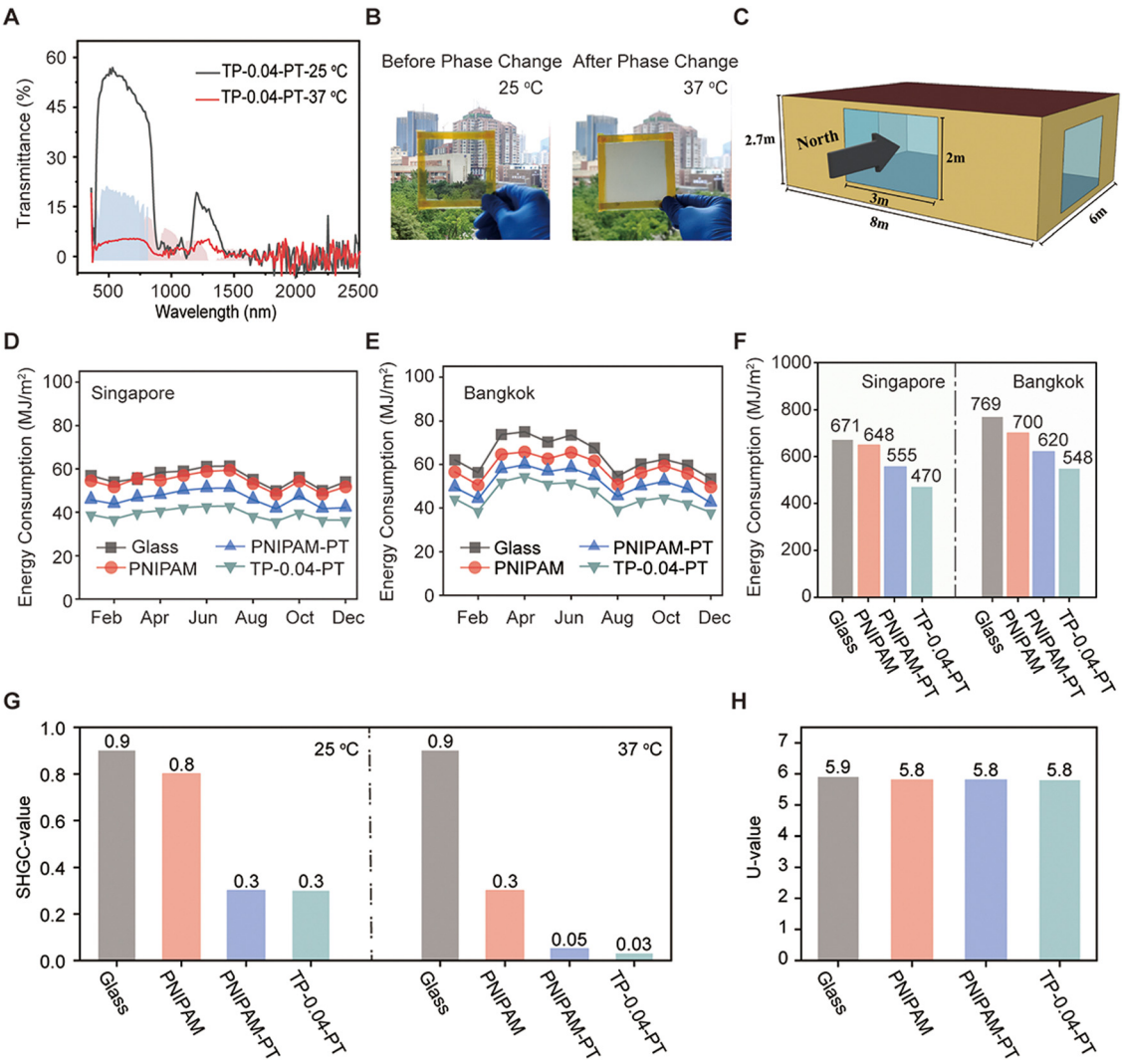

Fig. 2 An exploration of the application of smart bulk hydrogel panels in smart windows. (A) Vis-NIR transmittance curves of TP-0.04-PT smart window at different temperatures. (B) The photos of the TP-0.04-PT smart window before (about 25 °C) and after phase change (about 37 °C). (C) Schematic diagram of the building model used in the simulation. Energy consumption of glass window, PNIPAM window, PNIPAM-PT window, and TP-0.04-PT window in the climate condition of (D) Singapore and (E) Bangkok. (F) Annual energy consumption in Singapore and Bangkok. (G) Solar heat gain coefficient (SHGC-values) and (H) thermal transmission coefficient (*U*-values) of different windows.

notable reduction in the forward scattering intensity, coupled with a significant enhancement in backward scattering (Fig. 1H). The improved backward scattering helps shield NIR at temperatures above the LCST.

We propose a set of characteristics for an ideal low-latitude building energy-saving smart window (Fig. S5, ESI†) that should not allow penetration in the NIR range (780–2500 nm) to avoid heating a room and having a high ε_{LWIR} (2.5–25 μm) to promote radiative cooling.[12,29–31] Furthermore, the dynamic switching of transmittance within the visible light (vis, 380–780 nm) range can effectively cater to the requirements for visual transparency during early morning and evening hours, while providing privacy screening during the daytime.

The future prospects for TP-0.04-PT in the realm of low-latitude smart windows appear promising (Fig. 2A). The TP-0.04-PT hydrogel panel exhibits an optimal response temperature of 28 °C, enabling modified devices to respond promptly within the comfortable room temperature range (22–28 °C). This smart hydrogel panel exhibits a shading capacity of approximately 95% and 99% in the NIR range before and after phase change, respectively, which blocks most of the solar radiation energy from entering the room. Compared to previous studies, the TP-0.04-PT hydrogel panel also excels in key performance areas (Fig. S6 and Table S3, ESI†). The infrared emissivity (ε_{LWIR}) value is consistently maintained around 85% and can continuously dissipate heat through radiative cooling (Fig. S7, ESI†). This hydrogel panel has flexible switching within the visible spectrum with high transparency at 25 °C and superior privacy protection capabilities at 37 °C (Fig. 2B). The TP-0.04-PT hydrogel panel exhibited stability when exposed to temperature fluctuations. Specifically, its transmittance remained stable after 400 cycles of exposure to high (37 °C) and low (25 °C) temperatures (Fig. S8, ESI†).

Using EnergyPlus software and the same building model (Fig. 2C and Table S1, ESI†), calculations were made to compare the energy performance of different windows in the building.[32] Taking Singapore and Bangkok as examples – both of which represent typical climates in low-latitude regions – the annual energy consumption for the TP-0.04-PT smart window amounts to 470 MJ m^{-2} and 548 MJ m^{-2} respectively, which is 30.0% and 28.7% lower than that of glass windows (Fig. 2D–F and Table S2, ESI†). When compared to PNIPAM and PNIPAM-PT windows, the TP-0.04-PT smart window also demonstrates a substantial edge in energy-saving performance.

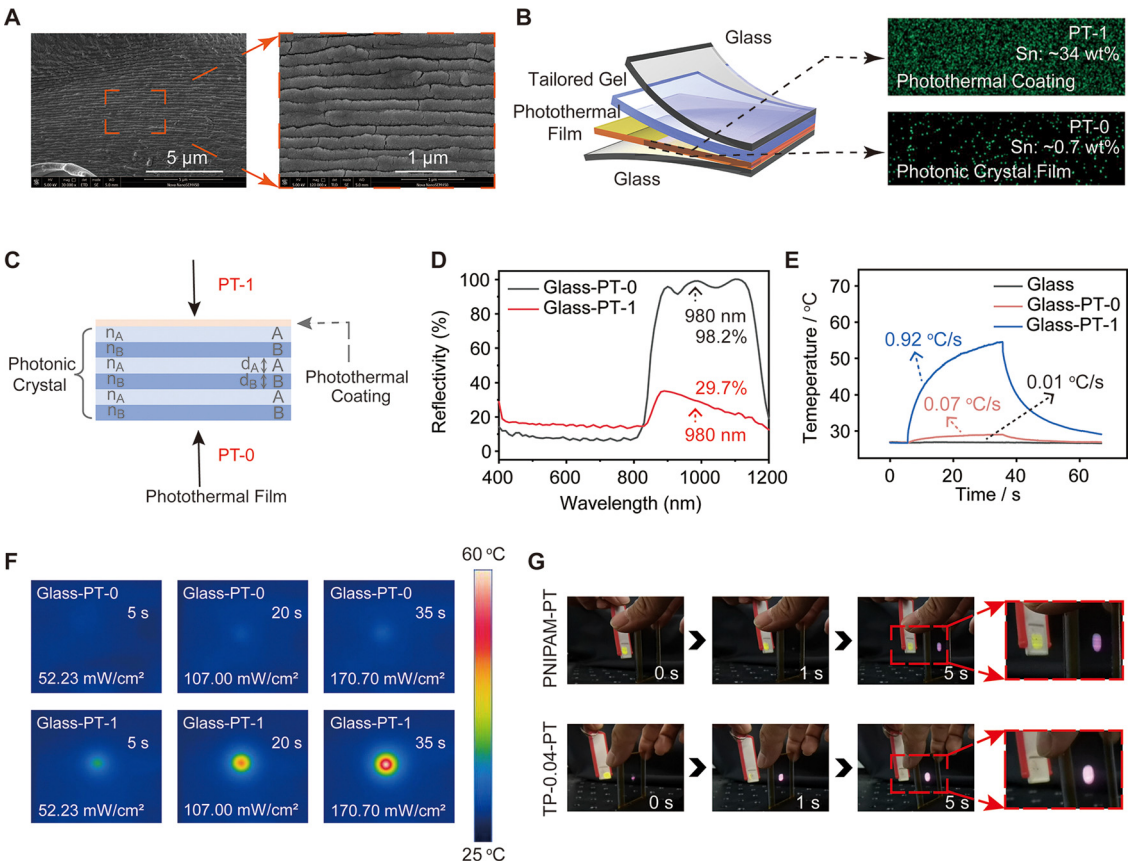

Fig. 3 The active local control performance of the smart bulk hydrogel panel. (A) Scanning electron microscopy (SEM) of PT film. (B) X-ray spectroscopy (EDS) of PT film from different testing directions. "−0" and "−1" represent different surfaces of the PT film, respectively. "−0" represents the direction of the photonic crystal layer. "−1" represents the direction of the photothermal coating. (C) The structure schematic of PT film. (D) Comparison of glass-PT-0 reflectance and glass-PT-1 reflectance. (E) and (F) The temperature change of glass-PT molds from different directions under 980 nm laser (170.7 mW cm^{-2}). (G) The response speed and clarity of different smart hydrogel panels to 980 nm laser (170.7 mW cm^{-2}).

To comprehensively evaluate the impact of the designed smart windows on the energy consumption of buildings, we compared the solar heat gain coefficient (SHGC-value) (Fig. 2G) and thermal transmission coefficient (*U*-value) (Fig. 2H) of different windows.[33,34] The SHGC value of the TP-0.04-PT smart window decreases from 0.3 to 0.03 compared to the glass window, proving it to be highly advantageous in reducing indoor heat accumulation, decreasing air conditioning loads, and enhancing overall energy efficiency. The *U*-values for glass windows and TP-0.04-PT smart windows are found to be 5.9 and 5.8, respectively, indicating they have similar heat transfer capabilities and insulation performance. The modified gel/PT film composite hydrogel panel presents a promising solution as an efficient and environmentally friendly smart window for buildings, facilitating energy conservation.

3.2. Active local control mode for smart information display

The PT film is composed of a photonic crystal layer (scanning electron microscopy (SEM) in Fig. 3A and Fig. S9, ESI†) and a photothermal coating (X-ray spectroscopy (EDS) in Fig. 3B), which provides a heat sourc.[35] When the NIR light reaches the PT film from the direction of the photothermal coating (PT-1) (Fig. 3C), it is partially absorbed, while the unabsorbed light is selectively reflected by the photonic crystal film, subsequently experiencing multiple absorptions and heat generation (Scheme 1B).[36,37] As a result, the reflectivity in the direction of the photothermal layer (glass-PT-1) is reduced from 98.2% to 29.7% as compared to the reflectivity in the direction of the photonic crystal layer (glass-PT-0) (Fig. 3D). The photothermal capabilities of the composite PT film glass molds (glass-PT) in the direction of the photothermal coating (glass-PT-1) are enhanced (Fig. 3E and F). Fig. S10 and S11 (ESI†) show that the photothermal capacity can be increased from 0.01 °C s^{-1} (glass) to 0.07 °C s^{-1} (glass-PT-0) and 0.92 °C s^{-1} (glass-PT-1), once the PT film adheres to the bare glass.

Due to the lower LCST (Fig. S12, ESI†) and higher photothermal efficiency (Fig. 3F), the TP-0.04-PT hydrogel panel exhibits a significantly improved active local control speed in response to the NIR laser (Fig. 3G). The appearance time for the scattering patterns of the TP-0.04-PT hydrogel panel is reduced to under 1 s, producing a milky white appearance with better "contrast". When the laser power is at 170.7 mW cm^{-2}, the excitation times for the 980 nm laser are defined as τ and $\tau_{1/2}$. The former is the time at which the relative transmittance of the panel in the visible range stabilizes (Fig. S13, ESI†), and the latter is the time at which it decreases to 50%. The dynamic switching rate of transmittance within the visible light spectrum of the TP-0.04-PT hydrogel panel accelerated significantly. In contrast to the pristine PNIPAM-PT hydrogel panel, the τ and $\tau_{1/2}$ of the TP-0.04-PT hydrogel panel reduced from 79.7 s and 16.8 s to 8.3 s and 1.8 s, respectively. In summary, the composite hydrogel panel exhibited high response speed, demonstrating its potential for smart information display.

In addition to response speed, increasing the contrast difference between phase change and non-phase change regions is important to enhance the clarity of the smart display. Specifically, the difference in the reflectance ($\Delta R_{@550nm}$) and the contrast ratio (eqn (1)) of relative transmittance (CR)

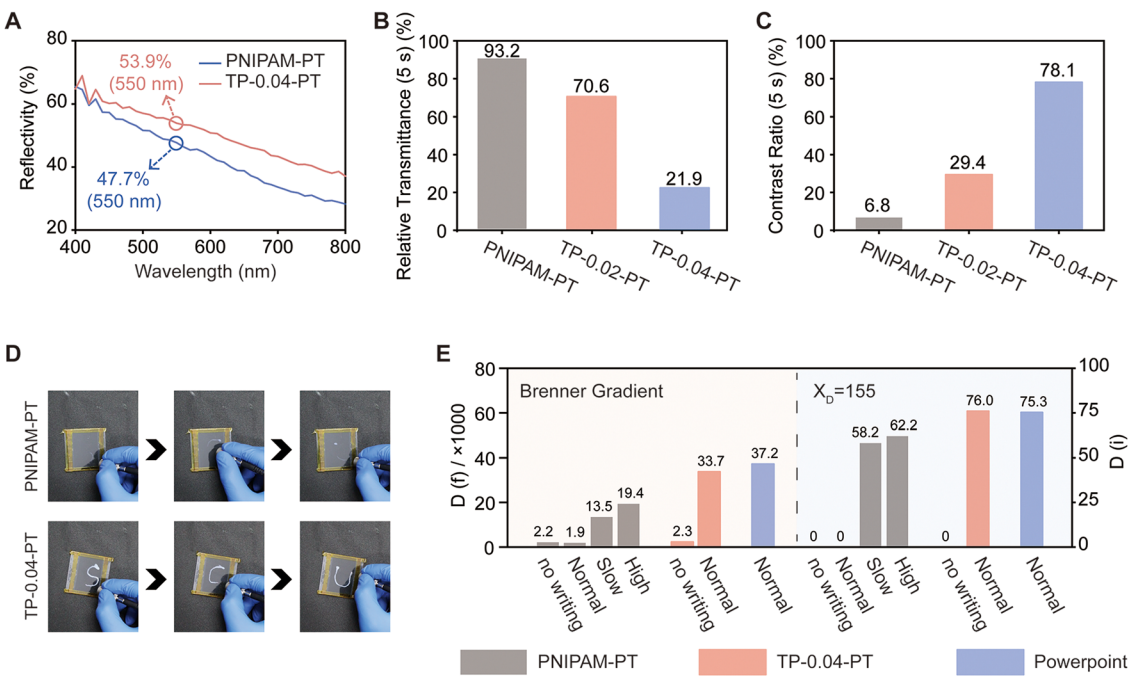

Fig. 4 (A) The reflectivity (37 °C) of the hydrogel panels (380–780 nm). (B) The relative transmittance (550 nm) of hydrogel panels at 5 s response (980 nm laser, 170.7 mW cm^{-2}). (C) The contrast ratio (CR) of various hydrogel panels was calculated from data from (B). (D) Digital photos of writing on information-displaying smart windows (980 nm, 640.1 mW cm^{-2}). (E) Comparison of writing clarity using the Brenner gradient (*D*(*f*)) and sharpness difference (*D*(*i*)) of the hydrogel panels.

between the phase-change and non-phase-change regions at 550 nm were used to evaluate the potential of hydrogel panels for smart information displays; this was done considering that the human eye is most sensitive to light at this wavelength.[38] The $R_{@550nm}$ of TP-0.04-PT hydrogel panel increased from 47.7% to 53.9% (Fig. 4A), and $\Delta R_{@550nm}$ increased from 35.5% to 41.4% compared with unmodified hydrogel panel (Fig. S15, ESI†). In response to laser excitation at 5 s (T_5), as compared with the PNIPAM-PT hydrogel panels, the CR of the TP-0.04-PT hydrogel panels increased from 6.7% to 78.1% (Fig. 4B and C), suggesting that the modified hydrogel panels feature higher clarity for smart displays.

$$\mathrm{CR} = \frac{T_0 - T_t}{T_0} \times 100\%, \quad (1)$$

where CR is the contrast ratio, indicating the imaging clarity. T_0 and T_t are the relative transmittance (550 nm) (Fig. S14, ESI†) of 0 s and t s, respectively.

The smart hydrogel panels were explored for applications in information displays (Fig. 4D and E). When the power density of the NIR laser is set to 640.1 mW cm^{-2}, instant writing can be achieved quickly (1.5 s per Byte) and repeatedly on the TP-0.04-PT hydrogel panel (Fig. 4D). In contrast, it is challenging to obtain distinct writing marks on the PNIPAM-PT hydrogel panel. Instant writing on the PNIPAM-PT hydrogel panel is achieved by either increasing the writing power (PNIPAM-PT-high, 853.5 mW cm^{-2}) or slowing down the writing speed (PNIPAM-PT-slow, 6.0 s per Byte). Nevertheless, continuous laser heating might inflict significant damage to the PT films, which could impede multiple writing attempts (Video S1, ESI†).

The clarity of instant writing (Fig. S16, ESI†) is described by Brenner gradient ($D(f)$) (Fig. S17, ESI†) and the sharpness difference between light and dark regions ($D(i)$) (Fig. S18, ESI†), which represents the difference in the transition variation between the two interfaces, and the difference in the average gray value between the written and unwritten regions, respectively (Fig. 4E).[31,39] Compared with PNIPAM-PT-high ($D(f)$ = 19.4 × 1000, $D(i)$ = 62.2), the $D(f)$ (33.7 × 1000) and $D(i)$ (76.0) of TP-0.04-PT-normal increase about 55% and 22%, respectively, which is comparable to that of handwritten PowerPoint ($D(f)$ = 37.2 × 1000, $D(i)$ = 75.3) using the same color background (Fig. S19, ESI†). Furthermore, due to the enhanced post-phase transition reflectivity (Fig. 4A), the application potential of the TP-0.04-PT hydrogel panels in smart projection is enhanced (Fig. S20, ESI†). Distinct images in various patterns (apples, flowers, and trees) can be formed at the center of the 100 × 100 mm^2 information-displaying TP-0.04-PT hydrogel panels. We believe that these composite hydrogel panels hold significant promise for applications in instant writing and smart projection.

4. Conclusions

In this work, we successfully develop a bulk hydrogel panel by meticulously integrating a specially designed hydrogel coupled with composite photonic crystal PT film, which can address the two deficiencies of pristine hydrogel, *i.e.*, its insufficient near-infrared (NIR) shielding and active local control. The NIR modulation capability of the former is enhanced through the directional design based on Mie scattering theory, which synergizes with the NIR selective shielding of the latter, resulting in a NIR shielding value of 99% (780–2500 nm) for this hydrogel panel. When used in smart windows, composite hydrogel panels can reduce building energy consumption at low latitudes, *e.g.*, annual energy consumption in Singapore and Bangkok has been demonstrated to be potentially reduced by 30.0% and 28.7%, respectively, compared with glass windows. The lower LCST of tailored PNIPAM and the great photothermal efficiency of composite film contribute to a sensitive NIR laser active local control of modified bulk hydrogel panel, as well as improved contrast of reflectivity at 550 nm ($\Delta R_{@550nm}$) between the local phase transition area and the rest of the window, increasing the in smart display clarity.

Data availability

Data pertaining to this work are presented in the main manuscript and the ESI.† Additional relevant data are available from the corresponding author upon reasonable request.

Conflicts of interest

There are no conflicts to declare.

Acknowledgements

This work was supported by the National Natural Science Foundation of China (NSFC) [52173042], the Global STEM Professorship Scheme sponsored by the Government of the Hong Kong Special, Administrative Region and Chinese University Hong Kong Start Up Fund, and the Doctoral Fund of Qingdao University of Science & Technology [04112-1].

References

1 Z. Yu, Y. Ma, L. Mao, Y. Lian, Y. Xiao, Z. Chen and Y. Zhang, *Mater. Horiz.*, 2024, **11**, 207–216.
2 Y. Tao, X. Fang, H. Zhang, G. Zhang, J. Tu and L. Shi, *Energy Convers. Manage.*, 2022, **252**, 115058.
3 Q. Lei, L. Wang, H. Xie and W. Yu, *Build. Environ.*, 2022, **222**, 109407.
4 J. Pu, C. Shen, L. Lu, Y. Long, C. Zhang, Y. Shuai and S. A. Kalogirou, *Energy Convers. Manage.*, 2024, **299**, 117815.
5 A. Radwan, T. Katsura, S. Memon, A. A. Serageldin, M. Nakamura and K. Nagano, *Energy Convers. Manage.*, 2020, **215**, 112920.
6 S. Nundy, A. Mesloub, B. M. Alsolami and A. Ghosh, *J. Cleaner Prod.*, 2021, **301**, 126854.
7 N. Aste, M. Buzzetti, C. Del Pero, R. Fusco, F. Leonforte and D. Testa, *J. Cleaner Prod.*, 2019, **219**, 35–45.
8 W. Zhang, X. Wu, L. Xie, O. Zhao, J. Zhong, X. Zeng and R. Zou, *Build. Environ.*, 2023, **238**, 110381.

9 G. Li, J. Chen, Z. Yan, S. Wang, Y. Ke, W. Luo, H. Ma, J. Guan and Y. Long, *Mater. Horiz.*, 2023, **10**, 2004–2012.
10 J. Li, P. Gu, H. Pan, Z. Qiao, J. Wang, Y. Cao, W. Wang and Y. Yang, *Adv. Sci.*, 2023, **10**, 2206044.
11 C. Lin, J. Hur, C. Y. H. Chao, G. Liu, S. Yao, W. Li and B. Huang, *Sci. Adv.*, 2022, **8**, 7359.
12 Z. Zhang, L. Zhang, Y. Zhou, Y. Cui, Z. Chen, Y. Liu, J. Li, Y. Long and Y. Gao, *Chem. Rev.*, 2023, **123**, 7025–7080.
13 J.-W. Guo, C.-F. Wang, J.-Y. Lai, C.-H. Lu and J.-K. Chen, *J. Membr. Sci.*, 2021, **618**, 118732.
14 G. Agrawal and R. Agrawal, *Polymers*, 2018, **10**, 418.
15 Y. Guan and Y. Zhang, *Soft Matter*, 2011, **7**, 6375–6384.
16 X.-H. Li, C. Liu, S.-P. Feng and N. X. Fang, *Joule*, 2019, **3**, 290–302.
17 Y. Zhou, S. Wang, J. Peng, Y. Tan, C. Li, F. Y. C. Boey and Y. Long, *Joule*, 2020, **4**, 2458–2474.
18 Y. Ding, Y. Duan, F. Yang, Y. Xiong and S. Guo, *Chem. Eng. J.*, 2023, **460**, 141572.
19 Y. Ding, C. Zhong, F. Yang, Z. Kang, B. Li, Y. Duan, Z. Zhao, X. Song, Y. Xiong and S. Guo, *Appl. Energy*, 2023, **348**, 121598.
20 T.-T. Zhuang, Y. Liu, Y. Li, Y. Zhao, L. Wu, J. Jiang and S.-H. Yu, *Angew. Chem., Int. Ed.*, 2016, **55**, 6396–6400.
21 J. Tian, H. Peng, X. Du, H. Wang, X. Cheng and Z. Du, *J. Alloys Compd.*, 2021, **858**, 157725.
22 T. G. Hwang, M. Jeong, J. Park, Y. J. Jung, D.-H. Hwang, H. Kong, D. W. Cho and J. M. Park, *Chem. Eng. J.*, 2023, **468**, 143614.
23 M. Wang, X. Xing, I. F. Perepichka, Y. Shi, D. Zhou, P. Wu and H. Meng, *Adv. Energy Mater.*, 2019, **9**, 1900433.
24 A. Eklund, H. Zhang, H. Zeng, A. Priimagi and O. Ikkala, *Adv. Funct. Mater.*, 2020, **30**, 2000754.
25 S. Amrhein, S. Suhm and J. Hubbuch, *Eng. Life Sci.*, 2016, **16**, 532–537.
26 X. Zhao, T. Li, H. Xie, H. Liu, L. Wang, Y. Qu, S. C. Li, S. Liu, A. H. Brozena, Z. Yu, J. Srebric and L. Hu, *Science*, 2023, **382**, 684–691.
27 L. Xiong, Y. Wei, C. Chen, X. Chen, Q. Fu and H. Deng, *Nat. Commun.*, 2023, **14**, 6129.
28 M. Leng and Y. Long, *Nat. Sustainable*, 2023, **6**, 619–620.
29 J. Dong, Y. Peng, Y. Zhang, Y. Chai, J. Long, Y. Zhang, Y. Zhao, Y. Huang and T. Liu, *Nano-Micro Lett.*, 2023, **15**, 181.
30 L. Xie, X. Wang, X. Zou, Z. Bai, S. Liang, C. Wei, S. Zha, M. Zheng, Y. Zhou, O. Yue and X. Liu, *Small*, 2023, **19**, 2304321.
31 Y. Liu, Y. Zhang, T. Chen, Z. Jin, W. Feng, M. Li, L. Chen and C. Wang, *Adv. Funct. Mater.*, 2023, **33**, 2307240.
32 S. Wang, T. Jiang, Y. Meng, R. Yang, G. Tan and Y. Long, *Science*, 2021, **374**, 1501–1504.
33 N. A. Lantonio and M. Krarti, *Appl. Energy*, 2022, **328**, 120239.
34 W. Meng, A. J. J. Kragt, Y. Gao, E. Brembilla, X. Hu, J. S. van der Burgt, A. P. H. J. Schenning, T. Klein, G. Zhou, E. R. van den Ham, L. Tan, L. Li, J. Wang and L. Jiang, *Adv. Mater.*, 2024, **36**, 2304910.
35 K. Zhao, Y. Wang, S. Zhang and W. Niu, *Ind. Eng. Chem. Res.*, 2021, **60**, 11151–11160.
36 V. Morandi, F. Marabelli, V. Amendola, M. Meneghetti and D. Comoretto, *Adv. Funct. Mater.*, 2007, **17**, 2779–2786.
37 Y. Wu, H. Shen, S. Ye, X. Zhao, K. Zhang, J. Zhang and B. Yang, *Adv. Opt. Mater.*, 2018, **6**, 1701262.
38 S. Sarwar, S. Park, T. T. Dao, M.-S. Lee, A. Ullah, S. Hong and C.-H. Han, *Sol. Energy Mater. Sol. Cells*, 2020, **210**, 110498.
39 S. Yazdanfar, K. B. Kenny, K. Tasimi, A. D. Corwin, E. L. Dixon and R. J. Filkins, *Opt. Express*, 2008, **16**, 8670–8677.